International Journal of
Molecular Sciences

MDPI

Review

Intracellular Cl^- Regulation of Ciliary Beating in Ciliated Human Nasal Epithelial Cells: Frequency and Distance of Ciliary Beating Observed by High-Speed Video Microscopy

Makoto Yasuda [1,*], Taka-aki Inui [1], Shigeru Hirano [1], Shinji Asano [2,3], Tomonori Okazaki [3], Toshio Inui [2,4], Yoshinori Marunaka [2,5,6] and Takashi Nakahari [2,*]

1 Department of Otolaryngology-Head and Neck Surgery, Graduate School of Medical Science, Kyoto Prefectural University of Medicine, Kyoto 602-8566, Japan; inui1227@koto.kpu-m.ac.jp (T.-a.I.); hirano@koto.kpu-m.ac.jp (S.H.)
2 Research Unit for Epithelial Physiology, Research Organization of Science and Technology, BKC, Ritsumeikan University, Kusatsu 525-8577, Japan; ashinji@ph.ritsumei.ac.jp (S.A.); t-inui@saisei-mirai.or.jp (T.I.); marunaka@koto.kpu-m.ac.jp (Y.M.)
3 Department of Molecular Physiology, Faculty of Pharmaceutical Sciences, BKC, Ritsumeikan University, Kusatsu 525-8577, Japan; ph0034fe@ed.ritsumei.ac.jp
4 Saisei Mirai Clinics, Moriguchi 570-0012, Japan
5 Department of Molecular Cell Physiology, Graduate School of Medical Science, Kyoto Prefectural University of Medicine, Kyoto 602-8566, Japan
6 Research Institute for Clinical Physiology, Kyoto Industrial Health Association, Kyoto 604-8472, Japan
* Correspondence: myasu@koto.kpu-m.ac.jp (M.Y.); nakahari@fc.ritsumei.ac.jp (T.N.); Tel.: +81-75-251-5603 (M.Y.); +81-77-561-3488 (ext. 7554) (T.N.)

Received: 11 May 2020; Accepted: 3 June 2020; Published: 5 June 2020

Abstract: Small inhaled particles, which are entrapped by the mucous layer that is maintained by mucous secretion via mucin exocytosis and fluid secretion, are removed from the nasal cavity by beating cilia. The functional activities of beating cilia are assessed by their frequency and the amplitude. Nasal ciliary beating is controlled by intracellular ions (Ca^{2+}, H^+ and Cl^-), and is enhanced by a decreased concentration of intracellular Cl^- ($[Cl^-]_i$) in ciliated human nasal epithelial cells (cHNECs) in primary culture, which increases the ciliary beat amplitude. A novel method to measure both ciliary beat frequency (CBF) and ciliary beat distance (CBD, an index of ciliary beat amplitude) in cHNECs has been developed using high-speed video microscopy, which revealed that a decrease in $[Cl^-]_i$ increased CBD, but not CBF, and an increase in $[Cl^-]_i$ decreased both CBD and CBF. Thus, $[Cl^-]_i$ inhibits ciliary beating in cHNECs, suggesting that axonemal structures controlling CBD and CBF may have Cl^- sensors and be regulated by $[Cl^-]_i$. These observations indicate that the activation of Cl^- secretion stimulates ciliary beating (increased CBD) mediated via a decrease in $[Cl^-]_i$ in cHNECs. Thus, $[Cl^-]_i$ is critical for controlling ciliary beating in cHNECs. This review introduces the concept of Cl^- regulation of ciliary beating in cHNECs.

Keywords: nasal cilia; intracellular Cl^- concentration; Cl^- channels; CFTR; mucociliary clearance

1. Introduction

The nasal and sinonasal epithelia are exposed to small inhaled airborne particles, such as allergens, chemicals, viruses and bacteria, which are removed via mucociliary clearance. Mucociliary clearance is a host defence mechanism of the respiratory tracts that comprises a thin mucous film and beating cilia [1–5]. In this process, small inhaled particles are entrapped by the thin mucous film (surface

mucous layer) and swept away from the nasal cavity by the activity of the beating cilia. Mucociliary clearance can be compared with a conveyer-belt system that extrudes the small inhaled particles from airways; that is, the surface mucous layer is the belt and the beating cilia are the engine for driving mucociliary clearance. Thus, the beating cilia are essential to maintain healthy nasal and sinonasal mucosa and to prevent their dysfunction, such as in primary ciliary dyskinesia (PCD) or induced sinusitis [1–6]. Therefore, drugs stimulating ciliary beating are of particular importance to improve or prevent nasal and sinonasal diseases.

The functional activities of ciliary beating can be assessed by two parameters, ciliary beat frequency (CBF) and waveform [6–14]. Previous studies have shown that CBF is a key parameter controlling the rate of mucociliary clearance [6,7]. However, there is evidence that the waveform is also an important factor for assessing the functional activities of the cilia [8–12]. There are several parameters for the assessment of waveform [8–12], one of which is the amplitude of ciliary beating. Studies of airway and nasal ciliary cells have demonstrated that the amplitude of ciliary beating is an essential factor for ciliary transport [14–16]. An increase in ciliary bend angle (CBA), which is an index of ciliary beat amplitude, has been shown to enhance the transport of microbeads on the airway surface driven by beating cilia [14]. Moreover, various stimulations have increased CBA in addition to CBF [14,17–21]. Recently, we developed a novel method for measuring ciliary beat distance (CBD), another index of ciliary beat amplitude, using a planar sheet of ciliated human nasal epithelial cells (cHNECs) in primary culture [15,16,20,21].

The intracellular Cl^- concentration ($[Cl^-]_i$) has been demonstrated to regulate cellular functions in various cell types, such as Na^+-permeable channels in foetal lung cells [22] and salivary ducts [23], Ca^{2+}-regulated exocytosis and Ca^{2+}-permeable channels in antral mucous cells [24], G-proteins [25], the cell cycle [26,27], tubulin polymerisation [28–30] and gene expression [31]. Moreover, a decrease in $[Cl^-]_i$ in airway ciliary cells, including cHNECs, has been shown to enhance CBD or CBA [15,16,20,21,32].

We recently demonstrated that daidzein and carbocisteine (CCis), which are activators of Cl^- channels, enhanced CBD mediated via a decrease in $[Cl^-]_i$ [15,16], suggesting that nasal secretion of Cl^- controls ciliary beating via $[Cl^-]_i$. At present, there are no known molecular targets of $[Cl^-]_i$ in airway ciliary cells or cHNECs. However, there is evidence that $[Cl^-]_i$ controls ciliary beating in cHNECs. In this review, we introduce the concept of Cl^- regulation of ciliary beating in cHNECs.

2. cHNECs

cHNECs isolated from nasal samples obtained during surgery or by brushing are cultured at the air–liquid interface (ALI) to differentiate into ciliated cells. cHNECs are widely used for cilia research [33–37]. Recent studies have demonstrated that cHNECs have some characteristic features that differ from ciliated airway cells of the trachea or lung. The ciliated tracheal and lung cells are sensitive to intracellular pH (pH_i); a high pH_i increases CBF, and a low pH_i decreases CBF [15,16,20,21,38]. The pH_i can be changed by switching from a CO_2/HCO_3^--containing to a CO_2/HCO_3^--free solution, although the changes in pH_i are small. H^+ is produced from CO_2 by carbonic anhydrase. Therefore, the switch to a CO_2/HCO_3^--free solution increases pH_i, and the return to a CO_2/HCO_3^--containing solution decreases it [15,16,20,21,38,39]. In tracheal ciliary cells, the switch to a CO_2/HCO_3^--free solution has been shown to increase CBF, mediated via an increase in pH_i [38]. However, in cHNECs, the switch to a CO_2/HCO_3^--free solution induced only a small and transient increase in pH_i, leading to a slight or sometimes no increase in CBF [15,16,21]. We also applied the NH_4^+ pulse to change pH_i. An application of the NH_4^+ pulse (an addition of NH_4Cl, such as 25 mM) in extracellular fluid releases a small amount of NH_3, which enters cells and traps H^+ to produce NH_4^+ leading to an increase in pH_i [21,38,39], and it induced a larger increase in pH_i independent of CO_2 than that induced by the CO_2/HCO_3^--free solution. In cHNECs, the NH_4^+ pulse induced transient CBF and pH_i increases. However, in the presence of acetazolamide (an inhibitor of carbonic anhydrase, which inhibits H^+ production from CO_2), it induced sustained increases, not transient, in pHi and CBF. These results indicate that cHNECs

produce a large amount of H^+, even under CO_2/HCO_3^--free conditions. A high level of H^+ production suggests a high CO_2 production or a high carbonic anhydrase activity in cHNECs.

Moreover, mouse nasal ciliary cells, unlike airway ciliary cells, have shown spontaneous CBF oscillation induced by periodic intracellular Ca^{2+} ($[Ca^{2+}]_i$) spikes and no increase in CBF during isobutylmethylxanthine (IBMX, an inhibitor of phosphodiesterase) stimulation [40]. Thus, cHNECs possess characteristic features distinct from tracheal or lung airway ciliary cells.

The characteristic features of cHNECs distinct from trachea and lung airway ciliary cells appear to be caused by the different embryological origins. The cHNECs are derived from the surface ectoderm, while ciliary cells of trachea and lung are from the endoderm. These characteristic features appear to be beneficial for cHNECs, which are exposed to air directly. In particular, a high H^+ production in cHNECs prevents pH_i changes induced by fluctuations in CO_2 concentrations during inspiration and expiration (0.3–40 mmHg).

A decrease in $[Cl^-]_i$ increases the amplitude, CBA or CBD, but not CBF, in cHNECs [15,16,21], similar to airway ciliary cells [20]. These observations suggest that $[Cl^-]_i$ is an important ion involved in regulating ciliary beating in airway ciliary cells, including cHNECs.

3. Analysis of Ciliary Beating in cHNECs

Primary cHNEC cultures are grown at the ALI and form a cell sheet similar to nasal or sinonasal epithelia. The ciliary beating of cHNECs can be observed from the apical side using high-speed video microscopy (HSVM). Since CBA measurement is difficult in the apical view, a new parameter is required to assess the amplitude of ciliary beating. Recently, CBD has been proposed as a new parameter for assessing the amplitude using HSVM and an image analysis programme.

3.1. HSVM

Recent developments in HSVM have allowed the observation of fine movements of airway ciliary beating, the analysis of which has enabled the measurement of the functional parameters of ciliary beating, not only the CBF but also the waveform or the beating pattern, including amplitude [9–11]. HSVM has been shown to be an effective tool for PCD diagnosis [11,41].

CBF has been established as the functional parameter of ciliary beating. However, there is no standard definition or consistency in the evaluation of ciliary waveforms, and the quantitative assessment of the waveform or of the pattern of ciliary beating remains controversial because of the waveform's complexity [11]. In our studies, the amplitude measured as CBD or CBA was shown to be an important factor in stimulating airway ciliary transport [4–12] and is proposed as a parameter for assessing the ciliary waveform.

Fine images of beating cilia with a high resolution in space and time are essential to measure the frequency and amplitude, and HSVM is a useful tool for this purpose. To observe ciliary beating, an inverted microscope with phase-contrast or differential interference contrast (DIC) optics as well as a high magnification objective lens (i.e., 60× or 100×) are suitable. However, the level of magnification should be selected according to the experimental purpose. The beating cilia move at a depth 5–20 μm above the apical surface of ciliary cells, and the focal plane depth of a high magnification lens with phase-contrast or DIC optics is <5 μm. In our experiments, we sometimes used HSVM equipped with a 60× objective lens without DIC or phase-contrast equipment for observing whole ciliary movements. Moreover, considering that a microscope light source may occasionally be insufficient for HSVM, especially when using DIC optics, a suitable optic, such as phase-contrast, was required. Given that CBF is highly temperature-dependent [3], a temperature-controlled micro-perfusion chamber was also necessary.

HSVM allows beating cilia from isolated ciliary cells to be viewed from three directions—a sideways profile, beating toward the lens (vertical direction), and from above [12]. However, in a sheet of cultured cells, such as cHNECs, most cells are viewed from the apical side (Figure 1A,B). CBF can be

measured in images recorded from all directions. However, it is difficult to measure CBD using the side view or vertical images, but an apical image is suitable for CBD measurement (Figures 1 and 2).

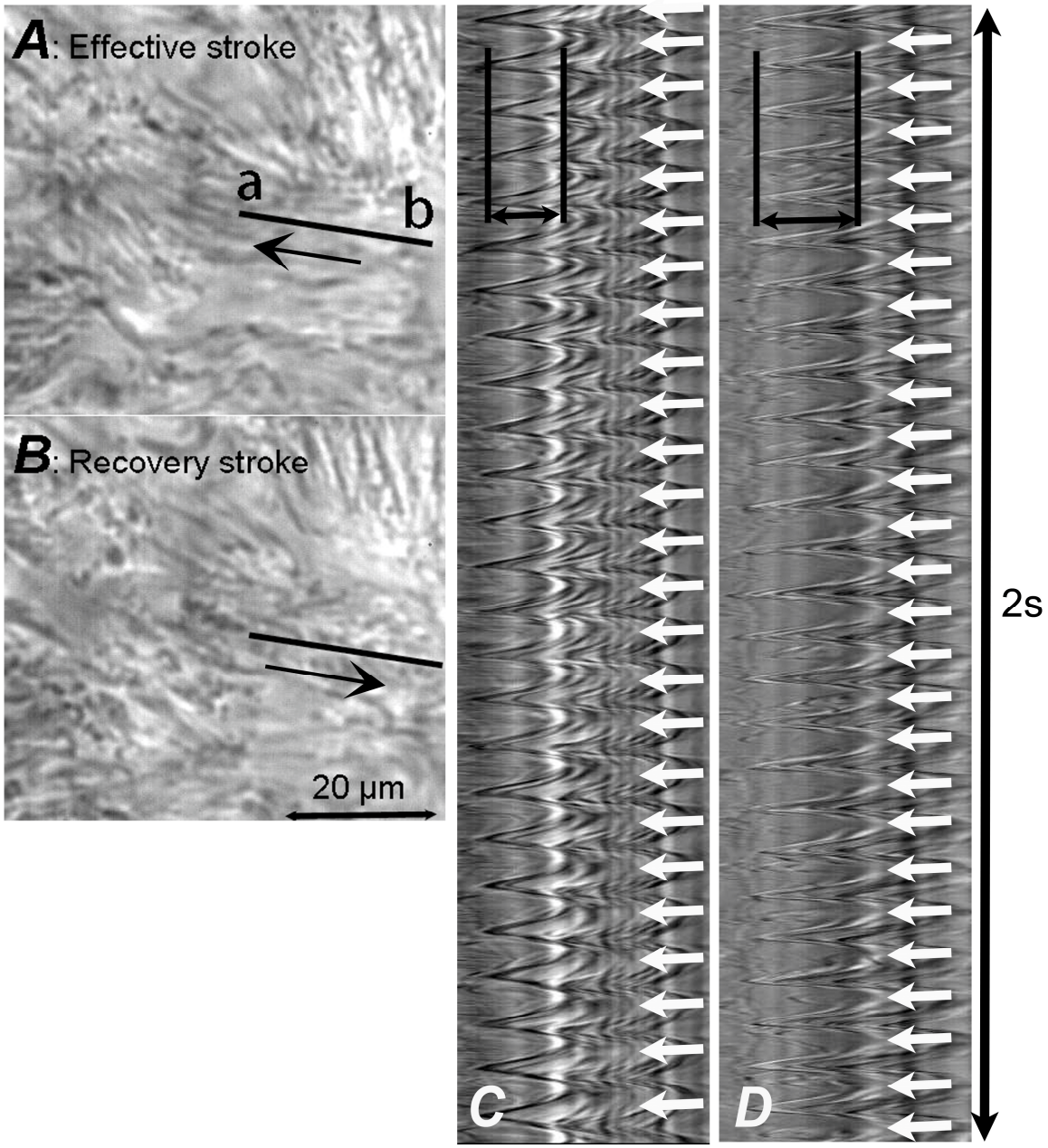

Figure 1. Video frame images of ciliated human nasal epithelial cells (cHNECs) recorded using high-speed video microscopy (500 fps) and images showing changes in the light intensity returned from the image analysis programme. (**A**,**B**) Video frame images of cHNECs. Panel A shows cilia in the end position of the effective stroke and the arrow shows the direction of the effective stroke, and Panel B shows cilia in the end position of the recovery stroke and the arrow shows the direction of the recovery stroke. (**C**) The light intensity changes for 2 s on line a–b marked in panel A. The distance between two lines marked by ←→ represents the ciliary beat distance (CBD), while the number of peaks marked by ↓ represents ciliary beat frequency (CBF, 12.5 Hz). (**D**) Light intensity changes of the ciliary beating in cHNECs during stimulation with 100 µM daidzein (13 Hz). The line was placed on the same position of a cHNEC as shown in panels A and B. The traces of light intensity changes clearly show that daidzein increases CBD, but not CBF.

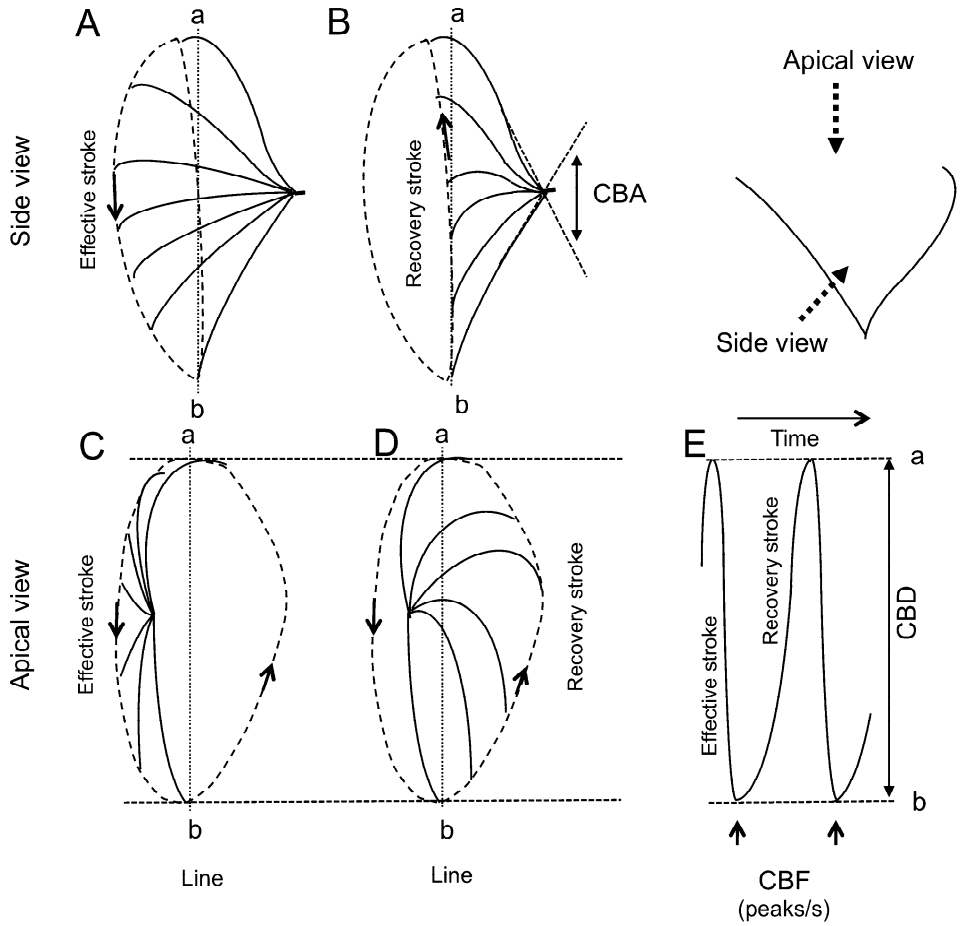

Figure 2. Schematic diagram of ciliary beating. The cilium travels in different planes during the effective and recovery strokes. During the effective stroke, the cilium tip moves in an arc with maximum speed in the plane perpendicular to the cell surface, and then, in the recovery stroke, the cilium swings back close to the cell surface. (**A**,**B**) Side view. Panels A and B show the effective stroke and the recovery stroke, respectively. The angle between the start and the end of the effective stroke is the ciliary beat angle (CBA, an index of ciliary beat amplitude). (**C**,**D**) Apical view. Panels C and D show the effective stroke and the recovery stroke, respectively. (**E**) The time course of changes in the light intensity of line a–b. To assess the amplitude of ciliary beating in the apical view, the distance between the start and the end of the effective stroke was measured. The measured distance is the ciliary beat distance (CBD, another index of ciliary beat amplitude). CBF, ciliary beat frequency.

3.2. Digital High-Speed Camera

Given their high frequency of 8–25 Hz at 37 °C, it is difficult to observe the fine movements of beating airway cilia at the National Television System Committee frame rate (30 fps). To visualise the complete cycle of ciliary beating, a high video recording rate (i.e., 500 Hz) is essential.

3.3. CBF Measurement

Available image analysis software for CBF measurement has been based on light intensity changes in the pixels of the recorded images over time (Figure 1). A semiautomated programme can determine CBF in selected lines of measured cilia [11]. At present, sample movements during perfusion occasionally introduce artefacts in the CBF obtained from the programme. Thus, while semiautomated CBF analysis has some advantages, such as a shorter time requirement, certain limitations are also present. When calculating CBF, light intensity peaks in the image obtained from the programme are counted (Figures 1 and 2).

3.4. CBD Measurement

Ciliary beating is coordinated with metachronal waves, which exhibit a whip-like movement. In the effective stroke of ciliary beating, the cilium tip makes an arc with a maximum speed in the plane perpendicular to the cell surface, while in the recovery stroke, the cilium swings back close to the cell surface (Figure 2). Studies have demonstrated that an abnormal waveform of ciliary beating induces ciliary dysfunction, leading to PCD, which is characterised by situs inversus totalis, sinusitis, and bronchiectasis [29]. The quantitative evaluation of ciliary waveform or ciliary wave pattern has been proposed to diagnose PCD based on an abnormal ciliary waveform or ciliary beat pattern [11,41]. Among the waveform evaluation parameters, we previously used CBD or CBA as an index of ciliary beat amplitude [4–10,24]. CBD has been characterised as the distance between the maximum forward and backward movements of the cilia tip [8–10,24,30,42] and CBA as the angle between the start and the end cilium positions in the effective stroke [4–8,24]. As shown in Figures 1 and 2, CBD and CBA are indices of ciliary beating amplitude and are thus the parameters for evaluating the ciliary beating waveform. It is certain that CBD or CBA are, at least, two of the most important parameters for evaluating the waveform of ciliary beating. Previous studies have demonstrated that an increase in CBA or CBD enhanced the transport of microbeads in the airway surface [4] or on the surface of cHNECs [9,10,24].

Moreover, in some cases, increases in CBD or CBA occurred without any increase in CBF. As mentioned above, a CBD increase alone enhanced microbead transport [9,10,24], although increases in CBF can also have this effect. Thus, CBD measurement is essential for evaluating the ciliary function in addition to CBF measurement.

Although various abnormal waveforms have been reported in PCD, the amplitude of ciliary beating, CBD and CBA, remain controversial as a parameter for PCD diagnosis [11]. However, CBD and CBA are important factors for evaluating normal airway cilia activity because an increase in CBD or CBA was shown to enhance microbead transport [14–16].

4. Changes in $[Cl^-]_i$

$[Cl^-]_i$ has been shown to modulate cellular functions in many cell types [22–32] and to be affected by cell volume changes. Many agonists activating ion transport, such as Cl^- secretion and K^+ release, have been demonstrated to evoke cell shrinkage under the isosmotic condition in many cell types [20,22,43–46]. This occurs when an increase in $[Ca^{2+}]_i$ or cyclic adenosine monophosphate accumulation stimulated by an agonist activates K^+ and Cl^- channels, leading to the cellular release of KCl [20,22,32,46]. The KCl release generates an osmotic gradient between the intracellular and extracellular space and is followed by a fluid efflux. Finally, the cell volume decreases to an equilibrium condition (isosmotic cell shrinkage). In airway epithelia, the activation of Cl^- secretion (Cl^- release from cells) also accompanies K^+ release for the maintenance of the intracellular electroneutrality. The KCl release, which generates a hypoosmotic condition in intracellular space, induces fluid efflux to evoke cell shrinkage [46]. Agonists, such as procaterol, CCis and daidzein, have already been shown to stimulate cell shrinkage in airway ciliary cells and cHNECs [15,16,20,21]. Furthermore, this isosmotic cell shrinkage has been demonstrated to decrease $[Cl^-]_i$ in airway ciliary cells and cHNECs [15,16,21].

In general, K^+ and Cl^-, which are the main intracellular cation and anion, respectively, are membrane-permeable ions, because the cell membrane has ion transporters and channels for K^+ and Cl^-. The isosmotic cell shrinkage, which is caused by the KCl release, decreases $[Cl^-]_i$. Figure 3 shows the mechanism for decreasing $[Cl^-]_i$ induced by cell shrinkage using a model cell for the calculation of $[K^+]_i$ and $[Cl^-]_i$. In this model cell, we assume that intracellular K^+ concentration ($[K^+]_i$) and $[Cl^-]_i$ are 125 and 45 mM in unstimulated condition, respectively. Assuming that an agonist decreases cell volume by 20%, the $[K^+]_i$ is maintained at 125 mM, but $[Cl^-]_i$ decreases from 45 to 25 mM, as shown in Figure 3. Thus, in this model cell, the isosmotic cell shrinkage decreases $[Cl^-]_i$ without any change in $[K^+]_i$ (Figure 3) [46]. The calculation in this model cell indicates that the $[Cl^-]_i$ decrease occurs during cell shrinkage under physiological conditions.

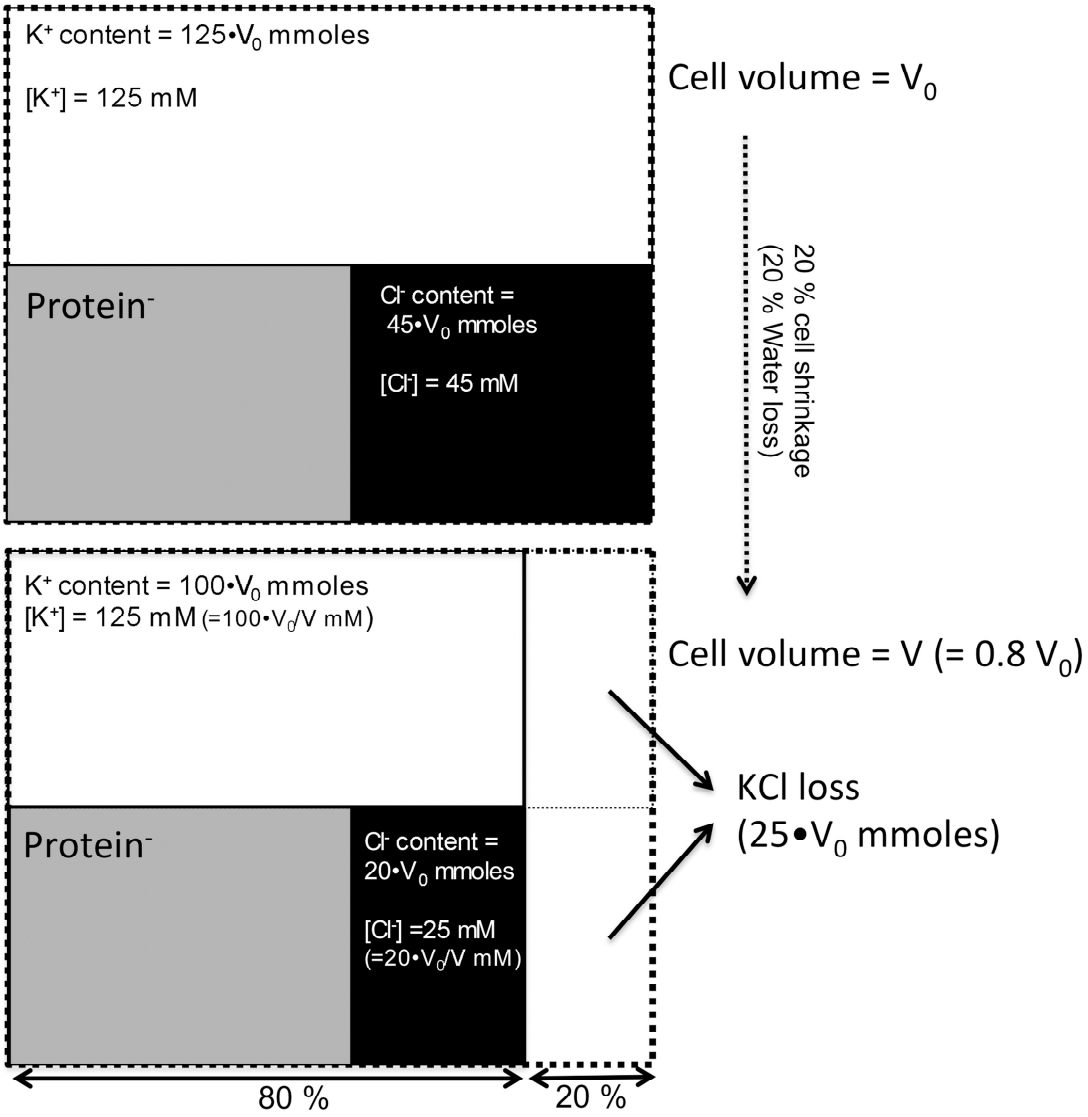

Figure 3. Decrease in $[Cl^-]_i$ induced by cell shrinkage under an isosmotic condition. In a model cell, $[K^+]_i$ and $[Cl^-]_i$ are 125 and 45 mM, respectively, in the unstimulated condition, while impermeable anions, such as proteins, maintain electroneutrality. Agonist stimulation activates K^+ or Cl^- channels or both, leading to KCl release. Assuming an agonist decreases cell volume by 20% (KCl release decreases cell volume from V_0 to V ($0.8 \bullet V_0$) under isosmotic conditions), the amount of KCl loss (mM) is $25 \bullet V_0$. The KCl release from the cell does not alter $[K^+]_i$, and it is maintained at 125 mM, but $[Cl^-]_i$ decreases to 25 mM. Thus, under isosmotic conditions, the cell shrinkage decreases only $[Cl^-]_i$ while maintaining $[K^+]_i$.

Daidzein is an agonist that stimulates Cl^- channels. It has been demonstrated to decrease only $[Cl^-]_i$, coupled with cell shrinkage, in cHNECs (Figure 4). This can be monitored using N-(ethoxycarbonylmethyl)-6-methoxyquinolinium bromide (MQAE), a Cl^- sensitive fluorescent dye. A decrease in $[Cl^-]_i$ increases the MQAE fluorescence intensity, whereas an increase in $[Cl^-]_i$ decreases it (Figure 4A,B) [15,16,20,21,47]. Daidzein, an agonist that stimulates Cl^- channels, has been shown to induce an $[Cl^-]_i$ decrease in cHNECs [15]. Figure 4A,B, in which cellular shapes have been superimposed on the MQAE fluorescence images, show changes in the cellular outline and MQAE fluorescence before and after daidzein stimulation. Daidzein stimulates cell shrinkage and increases the fluorescence intensity of MQAE. Relative changes in cell volume and MQAE fluorescence ratio (F_0/F) are shown in Figure 4C, where subscript "0" refers to the time when the stimulation was initiated.

Accordingly, daidzein decreased cell volume to 81% and F_0/F to 78%. In cHNECs, a decrease in $[Cl^-]_i$ (i.e., decreased cell volume) increased only CBD but not CBF (Figure 4D).

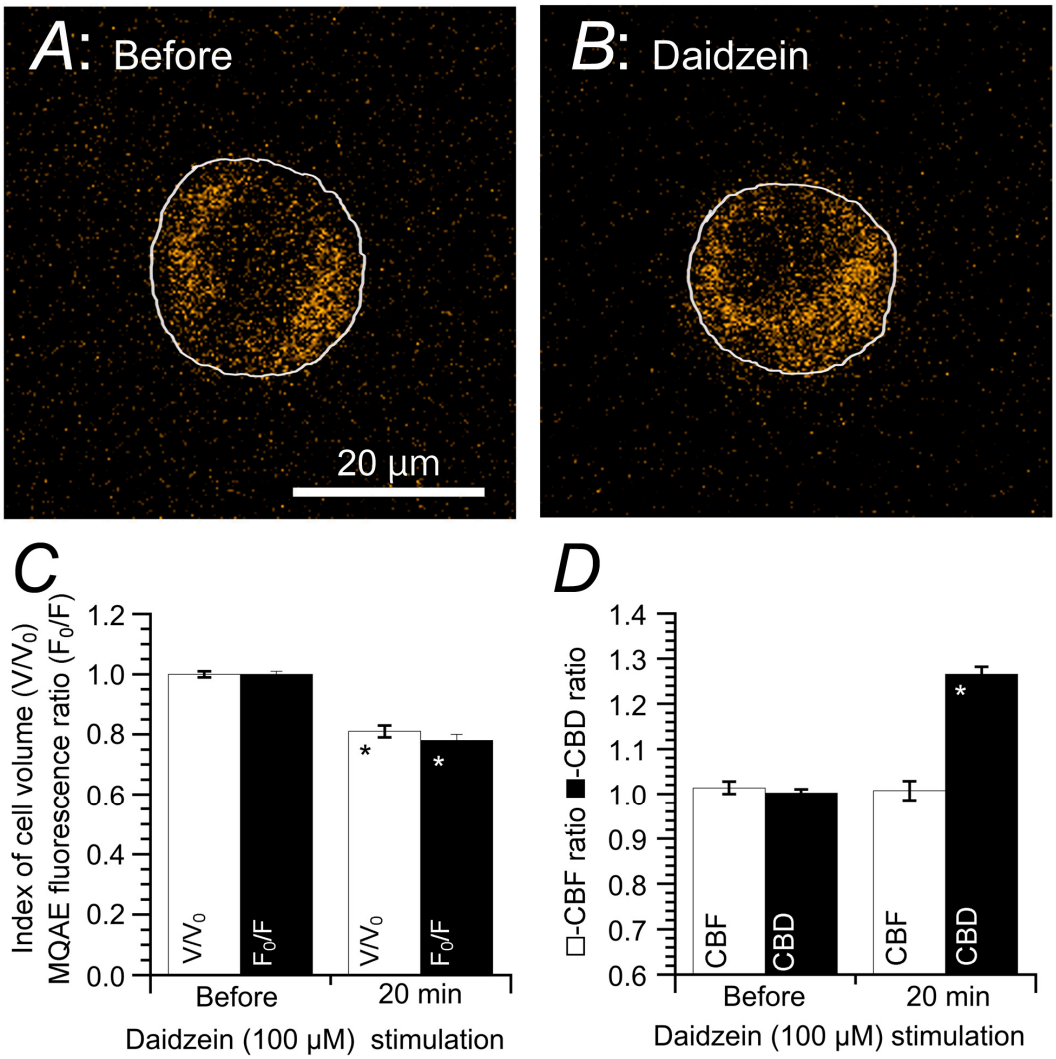

Figure 4. Changes in $[Cl^-]_i$ and cell volume following daidzein stimulation. Prior to daidzein (100 μM) stimulation, ciliated human nasal epithelial cells (cHNECs) were first perfused with a CO_2/HCO_3^--containing control solution for 5 min, followed by a CO_2/HCO_3^--free control solution for another 5 min. Then, a cell outline was superimposed on the N-ethoxycarbonylmethyl-6-methoxyquinolinium bromide (MQAE) fluorescence. (**A**) The MQAE fluorescent image of a cHNEC immediately prior to daidzein stimulation. (**B**) The MQAE fluorescent image of a cHNEC 20 min after daidzein stimulation (100 μM). Daidzein stimulation decreased cell volume and enhanced MQAE fluorescence intensity, indicating that daidzein decreased $[Cl^-]_i$ coupled with cell shrinkage. (**C**) Changes in MQAE fluorescence and cell volume. Daidzein decreased cell volume (V/V_0), leading to decreased $[Cl^-]_i$. (**D**) Changes in CBF and CBD during daidzein stimulation. Daidzein stimulation increased CBD but not CBF. * indicates results significantly different from the control values ($p < 0.05$). Error bars indicate SE. This figure was modified from Inui et al., 2018 [16] with permission.

5. $[Cl^-]_i$ Regulation of Ciliary Beating in cHNECs

5.1. Effects of Decreased $[Cl^-]_i$ on CBF and CBD

The effects of decreased $[Cl^-]_i$ on CBF and CBD are presented in Figure 5. A switch to a CO_2/HCO_3^--free solution alone decreased $[Cl^-]_i$ [15,16,21]. This $[Cl^-]_i$ decrease is explained by

the inhibition of NaCl entry via Na^+-HCO_3^- cotransporter (NBC) and Cl^-/HCO_3^- exchange (anion exchange, AE) in the CO_2/HCO_3^--free solution. Decreases in Cl^- entry by NBC and AE inhibition decreases $[Cl^-]_i$ and also increases CBD significantly, but not CBF. Experiments were performed under CO_2/HCO_3^--free conditions.

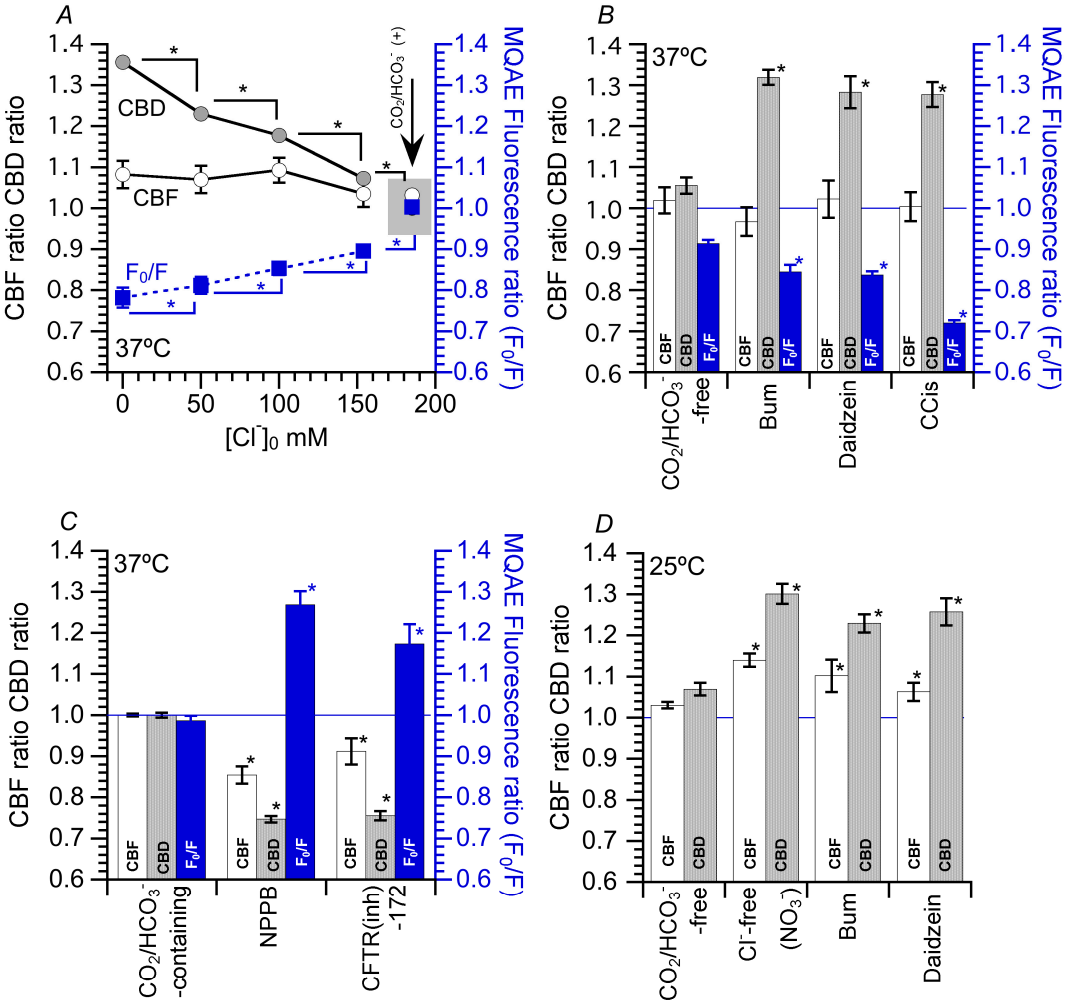

Figure 5. Effects of decreased intracellular Cl^- ($[Cl^-]_i$) on ciliary beat frequency (CBF) and ciliary beat distance (CBD). (**A**) Effects of Cl^--free (NO_3^-) solution on CBF, CBD and fluorescence ratio (F_0/F) of N-ethoxycarbonylmethyl-6-methoxyquinolinium bromide (MQAE). First, the perfusion solution was switched from a CO_2/HCO_3^--containing solution to a CO_2/HCO_3^--free solution. This switch decreased F_0/F (decrease in $[Cl^-]_i$) due to Na^+-HCO_3^- cotransporter and Cl^-/HCO_3^- exchange inhibition. The decreasing extracellular Cl^- concentration ($[Cl^-]_o$) decreased $[Cl^-]_i$. The decreased levels of F_0/F were dependent on $[Cl^-]_o$. The decreases in $[Cl^-]_i$ increased CBD, the levels of which are dependent on $[Cl^-]_i$. However, a decreased $[Cl^-]_i$ did not increase CBF. (**B**) Effects of bumetanide (bum), daidzein and carbocisteine (CCis) on CBF, CBD and F_0/F ($[Cl\text{-}]_i$). Experiments were performed in a CO_2/HCO_3^--free solution. Bum, daidzein and CCis decreased F_0/F, indicating decreases in $[Cl^-]_i$. These decreases in $[Cl^-]_i$ increased CBD, but CBF remained unchanged. (**C**) Effects of Cl^- channel blockers on CBF, CBD and F_0/F ($[Cl^-]_i$). 5-nitro-2-(3-phenylpropylamino)benzoic acid (NPPB) and a cystic fibrosis transmembrane conductance regulator inhibitor (CFTR(inh)-172) increased F_0/F ($[Cl^-]_i$). Increases in $[Cl^-]_i$ (F_0/F) decreased both CBF and CBD. (**D**) Effects of Cl^--free (NO_3^-) solution, bum, daidzein and CCis on CBF and CBD at 25 °C. Unlike at 37 °C, Cl^--free (NO_3^-) solution, bum, daidzein and CCis increased both CBF and CBD. Thus, a decrease in $[Cl^-]_i$ enhances both CBF and CBD at 25 °C. * indicates results significantly different from the control values ($p < 0.05$). Error bars indicate SE.

There are several methods to decrease $[Cl^-]_I$, including the substitution of Cl^- in the perfusion solution, inhibition of Cl^- entry and activation of Cl^- efflux. For Cl^- substitution, NO_3^- was used instead of Cl^- in the perfusion solution (Figure 5A). Decreasing extracellular Cl^- concentration ($[Cl^-]_o$) promoted a decrease in F_0/F in cHNECs, indicating a decrease in $[Cl^-]_i$. Values of F_0/F decreased according to $[Cl^-]_o$ decrease. In this experiment, F_0/Fs were set at four levels, dependent on $[Cl^-]_o$ in cHNECs, revealing that a decrease in $[Cl^-]_o$ decreases $[Cl^-]_i$. A decrease in $[Cl^-]_i$ with the application of NO_3^- solution increased CBD, but not CBF. Increases in CBD were dependent on decreases in $[Cl^-]_i$; a large decrease in $[Cl^-]_i$ induced a large increase in CBD (Figure 5A).

The effects of bumetanide (bum, an inhibitor of Na+/K+/2Cl- cotransporter (NKCC)), daidzein (an activator of Cl^- channels) and carbocisteine (CCis, an activator of Cl^- channels including cystic fibrosis transmembrane conductance regulator (CFTR)) on CBF and CBD under CO_2/HCO_3^--free conditions are shown in Figure 5B. The switch to CO_2/HCO_3^--free solution decreased $[Cl^-]_i$ as explained previously. Bum, which inhibits Na^+, K^+ and $2Cl^-$ entry, decreased F_0/F ($[Cl^-]_i$) (Figure 5B) [16,21]. An activation of Cl^- channels by daidzein or CCis also decreased $[Cl^-]_i$ (Figure 5B) [15,16]. Decreases in $[Cl^-]_i$ induced by NO_3^- solution, bum, daidzein and CCis increased CBD but not CBF.

5.2. Effects of Increase in $[Cl^-]_i$ on CBF and CBD

To increase $[Cl^-]_i$, the Cl^- channel inhibitor 5-nitro-2-(3-phenylpropylamino)benzoic acid (NPPB) was used. NPPB inhibits Cl^- release from cHNECs, leading to an increase in $[Cl^-]_i$. The addition of NPPB increased $[Cl^-]_i$ by inhibiting Cl^- release in cHNECs (Figure 5C). A similar increase in $[Cl^-]_i$ was induced by adding a cystic fibrosis transmembrane conductance regulator inhibitor (CFTR(inh)-172) to cHNECs [15]. Unlike a decrease in $[Cl^-]_i$, NPPB- and CFTR(inh)-172-induced increases in $[Cl^-]_i$ decreased both CBF and CBD. Thus, the range of $[Cl^-]_i$ activating CBF differed from that activating CBD.

5.3. Effects of Decrease in $[Cl^-]_i$ on CBF and CBD at 25 °C

A decrease in $[Cl^-]_i$ increased CBD, but not CBF, and an increase in $[Cl^-]_i$ decreased both CBF and CBD. However, a number of reports have suggested that a decrease in $[Cl^-]_i$ increases CBF [32,48–50]. These studies were performed at room temperature. The effects of decreased $[Cl^-]_i$ on CBF and CBA were examined at 25 °C (Figure 5D). The application of Cl^--free (NO_3^-) solution, bum or daidzein at 25 °C increased both CBF and CBD. These results suggest that a decrease in $[Cl^-]_i$ enhances both CBF and CBD, although the extent of the increases in CBF and CBD differed according to the temperature [16,20]. These results appear to suggest that $[Cl^-]_i$ may inhibit CBF and CBD and that the Cl^- concentration–response curve of CBF may shift to a higher concentration than that of CBD, indicating that the $[Cl^-]_i$ affects both CBF and CBD. The Cl^--binding affinity for the structures controlling CBD and CBF may depend on different temperatures.

5.4. Effects of Increased CBD on the Microbead Movement in cHNECs

To examine the effects of an increase in CBD on ciliary transport, microbeads were applied to cHNECs [14–16]. Microbeads reaching the surface of cHNECs were moved by the surface fluid flow driven by beating cilia. Microbead movement was observed using HSVM (60 fps). Figure 6A shows the movement of a microbead that reached the surface of a cHNEC (before daidzein addition). The large arrows show the positions of a microbead reaching the cell surface, while small arrows show the distance moved in 33 ms (over two frames). Figure 6B shows video images 5 min after daidzein addition, which enhanced the distance that a microbead moved. Figure 6C shows the CBD ratio and microbead movement before and after the daidzein addition. Accordingly, the increase in CBD enhanced microbead movement. Figure 6D shows the CBD ratio and microbead movement before and after CCis addition. Similarly, CCis addition enhanced CBD and microbead movement. CCis has already been shown to increase only CBD, without increasing CBF. The aforementioned results show that an increase in CBD alone enhances microbead movement, suggesting that CBD, in addition to CBF, is an important parameter for assessing the functions of ciliary beating.

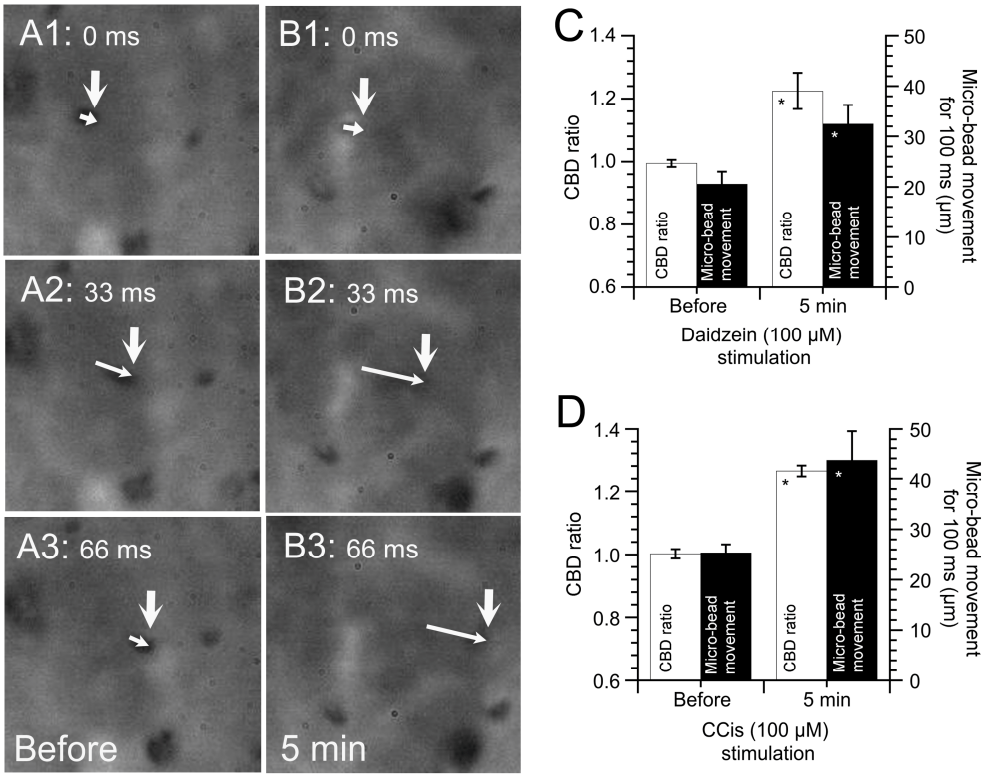

Figure 6. Latex microbead movement driven by ciliated human nasal epithelial cells. Panels A and B show six consecutive images recorded every 33 ms. (**A**) Before daidzein addition. (**B**) Five min after daidzein (100 μM) addition. The large arrows indicate the initial position of a microbead, and the small arrows indicate the distance that the microbead has moved. Daidzein stimulation enhanced microbead movement. (**C**) Daidzein-induced enhancement of ciliary beat distance (CBD) and microbead movement. Daidzein stimulation enhanced CBD and microbead movements. (**D**) Carbocisteine (CCis)-induced enhancement of CBD and microbead movements. CCis stimulation enhanced CBD and microbead movements. * indicates results significantly different from the control values ($p < 0.05$). Error bars indicate SE.

6. $[Cl^-]_i$ Modulation of CBF and CBD in cHNECs

Ciliary beating is maintained by force generated by molecular motors called dyneins [51]. Motile cilia can have two functionally distinct dyneins, outer dynein arms (ODAs), which control frequency, and inner dynein arms (IDAs), which control waveform, including CBD [52,53]. This suggests that a decrease in $[Cl^-]_i$ stimulates both ODA and IDA activity, whereas an increase in $[Cl^-]_i$ inhibits both. However, an $[Cl^-]_i$ decrease stimulates ODAs to increase CBF at 25 °C, but not at 37 °C. Based on these observations, axonemal structures controlling ODAs and IDAs might have a sensor to which $[Cl^-]_i$ binds. The binding of Cl^- to this sensor would decrease ODA and IDA activities, consequently decreasing CBF and CBD. The Cl^- concentration–response curve for CBF might shift to a higher concentration than that for CBD. The Cl^--binding affinity for the structures controlling the ODAs might become decreased at a low temperature, and if no Cl^- binds to the structures, ODA and CBF activity may increase. The Cl^--binding affinity for the structures controlling CBF might be higher than that controlling CBD.

There are numerous reports showing that $[Cl^-]_i$ modulates cellular functions in many cell types [22–27,31,54]. These observations suggest that cells have chloride sensors transducing this signal to the targets.

Piala et al. (2014) showed that $[Cl^-]_i$ binds to the kinase domain of with-no-lysine kinase (WNK) 1 and inhibits WNK1 autophosphorylation, inhibiting its activity [55]. WNK1–4 are serine/threonine protein kinases lacking a lysine residue within subdomain II of the kinase domain. They share a common

structure with >80% identity in their kinase domain [56,57], indicating that the chloride-binding site is conserved among the WNKs. Kinase studies have demonstrated that the affinities for Cl^- differ among WNK1, WNK3, and WNK4 [57,58]. WNK4 activity is inhibited when $[Cl^-]_i$ is 0–40 mM, while those of WNK1 and WNK3 become inhibited at 60–150 mM and 100–150 mM, respectively [57]. WNK1 and WNK4 have been shown to regulate CFTR [59] and NKCC1 of olfactory sensory cilia [60]. WNK4 has also been shown to regulate epithelial Na^+ channels (ENaC) in various tissues including airway [61,62]. CFTR and ENaC exist in nasal epithelia [15,16,63]. Moreover, WNK1 and WNK4 have been demonstrated to exist in olfactory sensory cilia [60]. Although the presence of WNK1 and WNK4 in motile cilia of cHNECs still remains uncertain, these observations may suggest that WNK1 and WNK4 are physiological $[Cl^-]_i$ sensors in cHNECs, as shown in an NCC study using WNK4 K/O mice [64]. Further studies are necessary.

WNK actions have been extensively studied in NaCl cotransporters (NCCs) of distal nephrons. WNK4 has been shown to inhibit epithelial Na^+ channels [61]. WNK1 and WNK4, which phosphorylate OSR1 (oxidative stress-responsive kinase 1) and SPAK (sterile20-related proline-, alanine-rich kinase), activate NKCC [65,66]. The inhibition of WNK1, WNK3 and WNK4, which depends on their affinities for Cl^-, have been shown to inhibit NCCs [66,67]. Thus, although WNK1, WNK3 and WNK4 are inhibited by Cl^-, WNK1 and WNK4 may be active in the physiological range of $[Cl^-]_I$ in many cell types, including cHNECs.

To examine the effects of $[Cl^-]_i$ on CBD and CBF in cHNECs, the relative changes in CBD and CBF (CBD ratio and CBF ratio), which were reported in previous studies [15,16,21], were plotted against the MQAE fluorescence ratio (F_0/F, an index of $[Cl^-]_i$) (Figure 7). CBD (red marks) was inhibited at a lower $[Cl^-]_i$ than CBF (blue marks). The inhibition of CBD and CBF by increasing $[Cl^-]_i$ seems to be similar to the inhibition of WNK4 and WNK1 obtained by increasing $[Cl^-]_i$ in the previous studies in vitro [55,57,58].

These studies may suggest that WNK4 exists in axonemal structures controlling IDAs and WNK1 exists in those controlling ODAs. The different subtypes of WNK, such as WNK4 or WNK1, may induce different actions in response to changes in $[Cl^-]_i$. Unfortunately, whether the axonemal structures controlling IDA and ODA possess WNK4 and WNK1 and the exact $[Cl^-]_i$ in cilia of cHNECs is unknown. If WNK4 and WNK1 exist in the axonemal structure controlling IDA and ODA, respectively, the effects of $[Cl^-]_i$ on CBF and CBA may be explained. For example, an $[Cl^-]_i$ decrease stimulated by cell shrinkage may activate WNK4, leading to the activation of IDA-controlling structures (CBD increase), but not WNK1, resulting in the continuing activation of the ODA-controlling structures (no CBF increase). A low temperature, such as room temperature, may decrease the affinities of WNK4 and WNK1 for Cl^-, leading to both WNK4 and WNK1 activation, which may increase CBD and CBF.

PCD patients have mutations in microtubule motor proteins and other structural proteins controlling ciliary beating. These proteins may have Cl^- sensors, such as WNK1and WNK4, and their activities may be affected by $[Cl^-]_i$. Their mutation may abolish activations of CBD and CBF in response to a decrease in $[Cl^-]_i$ and may make ciliary activities worse. Further studies are required.

A previous study showed that a decrease in $[Cl^-]_i$ increased the dynein affinity for microtubules [68]. Fluctuations in $[Cl^-]_i$, which modulate G proteins and GTPase [28,30,69], may also affect the interactions between tubulin and dyneins via G proteins and GTPase, which may change the sliding speed or force generation [70], leading to changes in CBF and CBD. These actions may also be mediated by WNK4 and WNK1 or be independent from them.

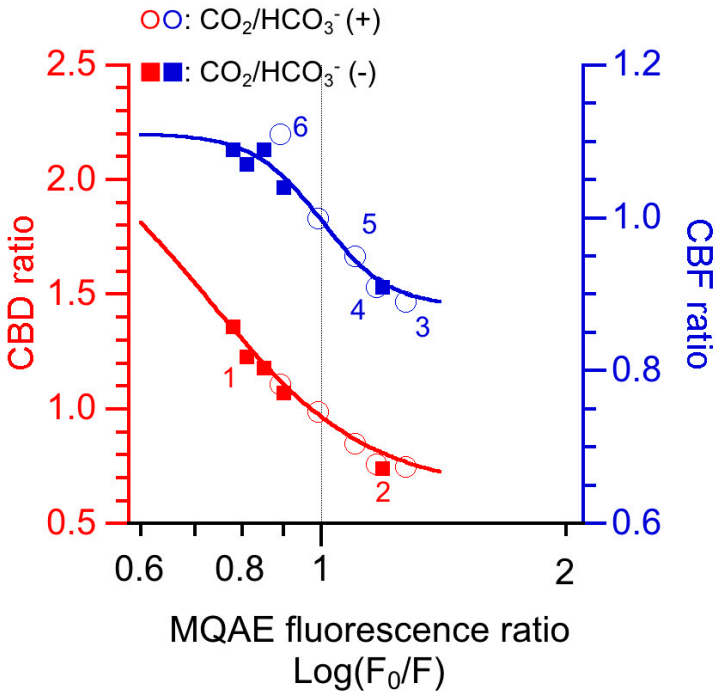

Figure 7. The effects of intracellular Cl^- ($[Cl^-]_i$) on relative changes in the ciliary beat distance (CBD) and ciliary beat frequency (CBF) (CBD ratio and CBF ratio) in cHNECs. $\{Cl^-\}_i$s are monitored using the N-(ethoxycarbonylmethyl)-6-methoxyquinolinium bromide (MQAE) fluorescence ratio (F_0/F). F_0/F is an index of $[Cl^-]_i$, not exact $[Cl^-]_i$. In this figure, the F_0/F, CBD ratios and CBF ratios have been published in previous experiments performed in both the presence and the absence of CO_2/HCO_3^- [15,16,21]. The closed squares labelled 1 were obtained from the Cl^--free (NO_3^-) solution experiments, and those labelled 2 were obtained from the 5-nitro-2-(3-phenylpropylamino)benzoic acid (NPPB) experiments. The open circles 3 and 4 were obtained from the NPPB and cystic fibrosis transmembrane conductance regulator inhibitor-172 experiments, respectively. The open circles 5 and 6 were obtained from the T16Ainh-A01 (a Ca^{2+}-activated Cl^- channel inhibitor) and the T16Ainh-A01 plus carbocisteine experiments, respectively. CBD was inhibited at a lower $[Cl^-]_i$ than CBF.

7. Conclusions

$[Cl^-]_i$ is an important signal ion that modulates ciliary beating in cHNECs. Nasal epithelia in primary culture have already shown to secrete Cl^- [63,71], although nasal mucosal glands including goblet cells also secrete Cl^- and mucins maintaining the nasal mucous layer. Under physiological conditions, Cl^- secretion in nasal epithelia maintains the surface serous fluid layer just below the mucous film, in which the cilia beat. Thus, Cl^- secretion in cHNECs maintains the mucociliary clearance in nasal and sinonasal epithelia. Our studies in cHNECs demonstrated that an activation of Cl^- secretion induces a decrease in $[Cl^-]_i$, which increases CBD. Moreover, airway cilia express CFTR [20]. Microdomains in the cilia are suggested to be isolated from the cell body, and their circumstances may be different from those of the cell body [17]. This may suggest that the activation or inhibition of CFTR induces a larger change in $[Cl^-]_i$ in the cilia than in the cell body. The summary of Cl^- regulation of ciliary beating in cHNECs is shown in Figure 8.

The drugs stimulating Cl^- secretion, such as CCis, improve the symptoms of nasal and sinonasal diseases by increasing CBD. Moreover, a decrease in $[Cl^-]_i$ may be a new therapeutic tool for improving nasal and sinonasal problems. However, the $[Cl^-]_i$ sensor of cHNECs remains unknown. We speculate WNK1 and WNK4 as candidates of the $[Cl^-]_i$ sensor controlling CBF and CBD. Nevertheless, the response of other kinases to an $[Cl^-]_i$ decrease must not be neglected. Further studies should provide elucidation.

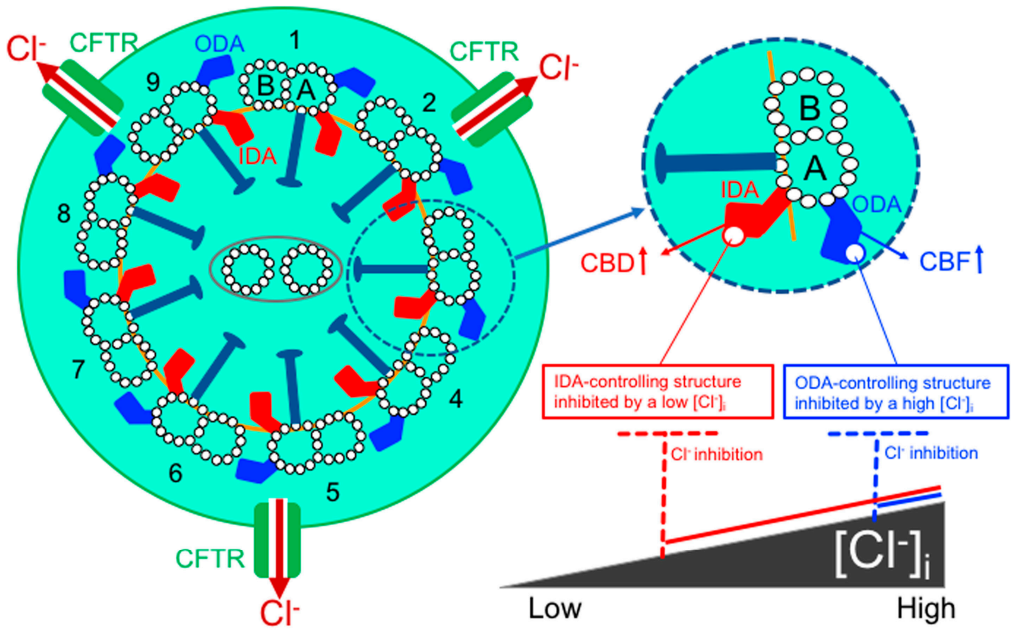

Figure 8. Cl^- modulation of ciliary beating in cHNECs. Ciliary membrane express CFTR [20]. Inner dynein arms (IDAs) control waveform including CBD and outer dynein arms (ODAs) control CBF. Axonemal structures controlling IDAs and ODAs appear to have Cl^- sensors. The sensors binding Cl^- may inhibit the axonemal structures controlling IDAs or ODAs leading to CBD decrease and CBF decrease. $[Cl^-]_i$ inhibiting IDA-controlling structures may be lower than that inhibiting ODA-controlling structures. Under the resting condition, ODAs are activated and IDAs are partly inactivated. At a lower $[Cl^-]_i$, ODAs continue to be active and IDAs are activated. At a higher $[Cl^-]_i$, both ODAs and IDAs are inactivated.

Author Contributions: Writing—original draft preparation, M.Y. and T.N.; writing—review, editing and discussion, T.I., Y.M., S.H. and S.A.; figure preparation, T.-a.I., M.Y., T.O. and T.N.; funding acquisition, Y.M. and M.Y. All authors have read and agreed to the published version of the manuscript.

Funding: This work was supported by Japan Society of the Promotion of Sciences to Y.M. (No. JP18H03182) and M.Y. (No. JP18K09325) and research funding to Y.M. from Saisei Mirai.

Acknowledgments: We would like to express our deepest gratitude to Osaka Medical College for allowing us to rent the digital high-speed video microscope. Experiments were carried out at Kyoto Prefectural University of Medicine (2018–2019) and Ritsumeikan University (2019).

Conflicts of Interest: The authors declare no conflict of interest.

References

1. Afzelius, B.A. Cilia-related diseases. *J. Pathol.* **2004**, *204*, 470–477. [CrossRef]
2. Wanner, A.; Salathe, M.; O'Riordan, T.G. Mucociliary clearance in the airways. *Am. J. Respir. Crit. Care Med.* **1996**, *154*, 1868–1902. [CrossRef]
3. Satir, P.; Christensen, S.T. Overview of Structure and Function of Mammalian Cilia. *Annu. Rev. Physiol.* **2007**, *69*, 377–400. [CrossRef] [PubMed]
4. Salathe, M. Regulation of mammarian ciliary beating. *Annu. Rev. Pysiol.* **2007**, *69*, 401–422. [CrossRef] [PubMed]
5. Tilley, A.E.; Walters, M.S.; Shaykhiev, R.; Crystal, R.G. Cilia dysfunction in lung disease. *Annu. Rev. Physiol.* **2015**, *77*, 379–406. [CrossRef] [PubMed]
6. Delmotte, P.; Sanderson, M.J. Ciliary Beat Frequency Is Maintained at a Maximal Rate in the Small Airways of Mouse Lung Slices. *Am. J. Respir. Cell Mol. Biol.* **2006**, *35*, 110–117. [CrossRef]
7. Toskala, E.; Nuutinen, J.; Rautiainen, M.; Torkkeli, T. The Correlation of Mucociliary Transport and Scanning Electron Microscopy of Nasal Mucosa. *Acta OtoLaryngol.* **1995**, *115*, 61–65. [CrossRef]

8. Chilvers, M.A.; Rutman, A.; O'Callaghan, C. Ciliary beat pattern is associated with specific ultrastructural defects in primary ciliary dyskinesia. *J. Allergy Clin. Immunol.* **2003**, *112*, 518–524. [CrossRef]
9. Raidt, J.; Wallmeier, J.; Hjeij, R.; Onnebrink, J.G.; Pennekamp, P.; Loges, N.T.; Olbrich, H.; Häffner, K.; Dougherty, G.W.; Omran, H.; et al. Ciliary beat patternand frequency in genetic variants of primary ciliary dyskinesia. *Eur. Respir. J.* **2014**, *44*, 1579–1588. [CrossRef]
10. Dy, F.J.; Midyat, L.; Wong, W.Y.; Boyer, D. Primary Ciliary Dyskinesia: Ciliary Beat Pattern/Frequency, Role of Molecular Analysis in the Diagnosis, and Neonatal Distress. *Am. J. Respir. Crit. Care Med.* **2016**, *193*, 689–691. [CrossRef]
11. Kempeneers, C.; Seaton, C.; Espinosa, B.G.; Chilvers, M.A. Ciliary functional analysis: Beating a path towards standardization. *Pediatr. Pulmonol.* **2019**, *54*, 1627–1638. [CrossRef]
12. Neesen, J.; Kirschner, R.; Ochs, M.; Schmiedl, A.; Habermann, B.; Mueller, C.; Holstein, A.F.; Nuesslein, T.; Adham, I.; Engel, W. Disruption of an inner arm dynein heavy chain gene results in asthenozoospermia and reduced ciliary beat frequency. *Hum. Mol. Genet.* **2001**, *10*, 1117–1128. [CrossRef] [PubMed]
13. Wood, C.R.; Hard, R.; Hennessey, T.M. Targeted gene disruption of dynein heavy chain 7 of Tetrahymena thermophile results in altered ciliary waveform and reduced swim speed. *J. Cell Sci.* **2007**, *120*, 3075–3085. [CrossRef]
14. Komatani-Tamiya, N.; Daikoku, E.; Takemura, Y.; Shimamoto, C.; Nakano, T.; Iwasaki, Y.; Kohda, Y.; Matsumura, H.; Marunaka, Y.; Nakahari, T. Procaterol-stimulated Increases in Ciliary Bend Amplitude and Ciliary Beat Frequency in Mouse Bronchioles. *Cell. Physiol. Biochem.* **2012**, *29*, 511–522. [CrossRef] [PubMed]
15. Inui, T.-A.; Yasuda, M.; Hirano, S.; Ikeuchi, Y.; Kogiso, H.; Inui, T.; Marunaka, Y.; Nakahari, T. Enhancement of ciliary beat amplitude by carbocisteine in ciliated human nasal epithelial cells. *Laryngoscope* **2020**, *130*, E289–E297. [CrossRef] [PubMed]
16. Inui, T.-A.; Yasuda, M.; Hirano, S.; Ikeuchi, Y.; Kogiso, H.; Inui, T.; Marunaka, Y.; Nakahari, T. Daidzein-Stimulated Increase in the Ciliary Beating Amplitude via an [Cl−]i Decrease in Ciliated Human Nasal Epithelial Cells. *Int. J. Mol. Sci.* **2018**, *19*, 3754. [CrossRef] [PubMed]
17. Kogiso, H.; Hosogi, S.; Ikeuchi, Y.; Tanaka, S.; Shimamoto, C.; Matsumura, H.; Nakano, T.; Sano, K.I.; Inui, T.; Marunaka, Y.; et al. A low [Ca2+]i-induced enhancement of cAMP-activated ciliary beating by PDE1Ainhibition in mouse airway cilia. *Pflügers Arch.* **2017**, *469*, 1215–1227. [CrossRef]
18. Kogiso, H.; Hosogi, S.; Ikeuchi, Y.; Tanaka, S.; Inui, T.; Marunaka, Y.; Nakahari, T. [Ca2+]i modulation of cAMP-stimulated ciliary beat frequency via PDE1 in airway ciliary cells of mice. *Exp. Physiol.* **2018**, *103*, 381–390. [CrossRef]
19. Kogiso, H.; Ikeuchi, Y.; Sumiya, M.; Hosogi, S.; Tanaka, S.; Shimamoto, C.; Inui, T.; Marunaka, Y.; Nakahari, T. Seihai-to (TJ-90)-Induced Activation of Airway Ciliary Beatings of Mice: Ca2+ Modulation of cAMP-Stimulated Ciliary Beatings via PDE1. *Int. J. Mol. Sci.* **2018**, *19*, 658. [CrossRef]
20. Ikeuchi, Y.; Kogiso, H.; Hosogi, S.; Tanaka, S.; Shimamoto, C.; Matsumura, H.; Inui, T.; Marunaka, Y.; Nakahari, T. Carbocisteine stimulated an increase in ciliary bend angle via a decrease in [Cl−]i in mouse airway cilia. *Pflügers Arch.* **2018**, *471*, 365–380. [CrossRef]
21. Inui, T.-A.; Murakami, K.; Yasuda, M.; Hirano, S.; Ikeuchi, Y.; Kogiso, H.; Hosogi, S.; Inui, T.; Marunaka, Y.; Nakahari, T. Ciliary beating amplitude controlled by intracellular Cl− and a high rate of CO2 production in ciliated human nasal epithelial cells. *Pflügers Arch.* **2019**, *471*, 1127–1142. [CrossRef] [PubMed]
22. Tohda, H.; Foskett, J.K.; O'Brodovich, H.; Marunaka, Y. Cl− regulation of a Ca2+-activated nonselective cation channel in β-aginist-treated fetal distal lung epithelium. *Am. J. Physiol. Cell Physiol.* **1994**, *266*, C104–C109. [CrossRef] [PubMed]
23. Dinudom, A.; Young, J.A.; Cook, D.I. Na+ and Cl? conductances are controlled by cytosolic Cl? concentration in the intralobular duct cells of mouse mandibular glands. *J. Membr. Biol.* **1993**, *135*, 289–295. [CrossRef] [PubMed]
24. Shimamoto, C.; Umegaki, E.; Katsu, K.-I.; Kato, M.; Fujiwara, S.; Kubota, T.; Nakahari, T. [Cl−]i modulation of Ca2+-regulated exocytosis in ACh-stimulated antral mucous cells of guinea pig. *Am. J. Physiol. Gastrointest. Liver Physiol.* **2007**, *293*, G824–G837. [CrossRef] [PubMed]
25. Higashijima, T.; Ferguson, K.M.; Sternweis, P.C. Regulation of hormone-sensitive GTP-dependent regulatory proteins by chloride. *J. Biol. Chem.* **1987**, *262*, 3597–3602.

26. Miyazaki, H.; Shiozaki, A.; Niisato, N.; Ohsawa, R.; Itoi, H.; Ueda, Y.; Otsuji, E.; Yamagishi, H.; Iwasaki, Y.; Nakano, T.; et al. Chloride ions control the G1/S cell-cycle checkpoint by regulating the expression of p21 through a p53-independent pathway in human gastric cancer cells. *Biochem. Biophys. Res. Commun.* **2008**, *366*, 506–512. [CrossRef]
27. Ohsawa, R.; Miyazaki, H.; Niisato, N.; Shiozaki, A.; Iwasaki, Y.; Otsuji, E.; Marunaka, Y. Intracellular chloride regulates cell proliferation through the activation of stress-activated protein kinases in MKN28 human gastric cancer cells. *J. Cell. Physiol.* **2010**, *223*, 764–770. [CrossRef]
28. Nakajima, K.-I.; Marunaka, Y. Intracellular chloride ion concentration in differentiating neuronal cell and its role in growing neurite. *Biochem. Biophys. Res. Commun.* **2016**, *479*, 338–342. [CrossRef]
29. Nakajima, K.-I.; Niisato, N.; Marunaka, Y. Enhancement of tubulin polymerization by Cl−-induced blockade of intrinsic GTPase. *Biochem. Biophys. Res. Commun.* **2012**, *425*, 225–229. [CrossRef]
30. Nakajima, K.-I.; Miyazaki, H.; Niisato, N.; Marunaka, Y. Essential role of NKCC1 in NGF-induced neurite outgrowth. *Biochem. Biophys. Res. Commun.* **2007**, *359*, 604–610. [CrossRef]
31. Niisato, N.; Eaton, D.C.; Marunaka, Y. Involvement of cytosolic Cl− in osmoregulation of α-ENaC gene expression. *Am. J. Physiol. Renal Physiol.* **2004**, *287*, F932–F939. [CrossRef] [PubMed]
32. Shiima-Kinoshita, C.; Min, K.-Y.; Hanafusa, T.; Mori, H.; Nakahari, T. β2-adrenergic regulation of ciliary beat frequency in rat bronchiolar epithelium: Potentiation by isosmotic cell shrinkage. *J. Physiol.* **2003**, *554*, 403–416. [CrossRef]
33. Lee, D.D.H.; Petris, A.; Hynds, R.E.; O'Callaghan, C. Ciliated Epithelial Cell Differentiation at Air-Liquid Interface Using Commercially Available Culture Media. *Methods Mol. Biol.* **2020**, *2109*, 275–291. [CrossRef]
34. Hirst, R.A.; Rutman, A.; Williams, G.; O'Callaghan, C. Ciliated air-liquid culturesas an aid to diagnostic testing of primary ciliary dyskinesia. *Chest* **2010**, *138*, 1441–1447. [CrossRef]
35. Hirst, R.A.; Jackson, C.L.; Coles, J.L.; Williams, G.; Rutman, A.; Goggin, P.M.; Adam, E.C.; Page, A.; Evans, H.J.; Lackie, P.M.; et al. Culture of primary ciliary dyskinesia epithelial cells at air-liquid interface can alter cilaiary phenotype but remains a robust and informative diagnostic aid. *PLoS ONE* **2014**, *9*, e89675. [CrossRef] [PubMed]
36. Müller, L.; Brighton, L.E.; Carson, J.L.; Fischer, W.A.; Jaspers, I. Culturing of Human Nasal Epithelial Cells at the Air Liquid Interface. *J. Vis. Exp.* **2013**, *80*, 50646. [CrossRef]
37. Schögler, A.; Blank, F.; Brügger, M.; Beyeler, S.; Tschanz, S.A.; Regamey, N.; Casaulta, C.; Geiser, T.; Alves, M.P. Characterization of pediatric cystic fibrosis airway epithelial cell cultures at the air-liquid interface obtained by non-invasive nasal cytology brush sampling. *Respir. Res.* **2017**, *18*, 215. [CrossRef] [PubMed]
38. Sutto, Z.; Conner, G.E.; Salathe, M. Regulation of human airway ciliary beat frequency by intracellular pH. *J. Physiol.* **2004**, *560*, 519–532. [CrossRef]
39. Tokuda, S.; Shimamoto, C.; Yoshida, H.; Murao, H.; Kishima, G.; Ito, S.; Kubota, T.; Hanafusa, T.; Sugimoto, T.; Niisato, N.; et al. HCO3−-dependent pHi recovery and overacidification induced by NH4+ pulse in rat lung alveolar typeII cells: HCO3−-dependent NH3 excretion from lungs? *Pflügers Arch.* **2007**, *455*, 223–239. [CrossRef]
40. Kuremoto, T.; Kogiso, H.; Yasuda, M.; Inui, T.-A.; Murakami, K.; Hirano, S.; Ikeuchi, Y.; Hosogi, S.; Inui, T.; Marunaka, Y.; et al. Spontaneous oscillation of the ciliary beat frequency regulated by release of Ca2+ from intracellular stores in mouse nasal epithelia. *Biochem. Biophys. Res. Commun.* **2018**, *507*, 211–216. [CrossRef]
41. Rubbo, B.; Shoemark, A.; Jackson, C.L.; Hirst, R.; Thompson, J.; Hayes, J.; Frost, E.; Copeland, F.; Hogg, C.; O'Callaghan, C.; et al. Accuracy of high-speed video analysis to diagnose primary ciliary dyskineasia. *Chest* **2019**, *155*, 1008–1017. [CrossRef]
42. Yaghi, A.; Dolovich, M.B. Airway Epithelial Cell Cilia and Obstructive Lung Disease. *Cells* **2016**, *5*, 40. [CrossRef] [PubMed]
43. Foskett, J.K.; Melvin, J.E. Activation of salivary secretion: Coupling of cell volume and [Ca2+]i in single cells. *Science* **1989**, *244*, 1582–1585. [CrossRef] [PubMed]
44. Nakahari, T.; Murakami, M.; Yoshida, H.; Miyamoto, M.; Sohma, Y.; Imai, Y. Decrease in rat submandibular acinar cell volume during ACh stimulation. *Am. J. Physiol. Liver Physiol.* **1990**, *258*, G878–G886. [CrossRef]
45. Fujiwara, S.; Shimamoto, C.; Katsu, K.-I.; Imai, Y.; Nakahari, T. Isosmotic modulation of Ca2+-regulated exocytosis in guinea-pig antral mucous cells: Role of cell volume. *J. Physiol.* **1999**, *516*, 85–100. [CrossRef]
46. Marunaka, Y. Hormonal and Osmotic Regulation of NaCl Transport in Renal Distal Nephron Epithelium. *Jpn. J. Physiol.* **1997**, *47*, 499–511. [CrossRef]

47. Ikeuchi, Y.; Kogiso, H.; Hosogi, S.; Tanaka, S.; Shimamoto, C.; Inui, T.; Nakahari, T.; Marunaka, Y. Measurement of [Cl−]i unaffected by the cell volume change using MQAE-based two-photon microscopy in airway ciliary cells of mice. *J. Physiol. Sci.* **2018**, *68*, 191–199. [CrossRef]
48. Zhang, S.; Smith, N.; Schuster, D.; Azbell, C.; Sorscher, E.J.; Rowe, S.M.; Woodworth, B.A. Quercetin increases cystic fibrosis transmembrane conductance regulator-mediated chloride transport and ciliary beat frequency: Therapeutic implications for chronic rhinosinusitis. *Am. J. Rhinol. Allergy* **2011**, *25*, 307–312. [CrossRef]
49. Zhang, S.; Skinner, D.; Hicks, S.B.; Bevensee, M.O.; Sorscher, E.J.; Lazrak, A.; Matalon, S.; McNicholas, C.M.; Woodworth, B.A. Sinupret Activates CFTR and TMEM16A-Dependent Transepithelial Chloride Transport and Improves Indicators of Mucociliary Clearance. *PLoS ONE* **2014**, *9*, e104090. [CrossRef]
50. Azbell, C.; Zhang, S.; Skinner, D.; Fortenberry, J.; Sorscher, E.J.; Woodworth, B.A.; Zhang, S.; Sorscher, E.J.; Woodworth, B.A. Hesperidin stimulates cystic fibrosis transmembrane conductance regulator-mediated chloride secretion and ciliary beat frequency in sinonasal epithelium. *Otolaryngol. Neck Surg.* **2010**, *143*, 397–404. [CrossRef]
51. Gibbons, I.R.; Rowe, A.J. Dynein: A protein with adenosine triohosphatase activity from cilia. *Science* **1965**, *149*, 424–426. [CrossRef] [PubMed]
52. Brokaw, C.J. Control of flagellar bending: A new agenda based on dynein diversity. *Cell Motil. Cytoskelet.* **1994**, *28*, 199–204. [CrossRef] [PubMed]
53. Brokaw, C.J.; Kamiya, R. Bending patterns of Chlamydomonas flagella: IV. Mutants with defects in inner and outer dynein arms indicate differences in dynein arm function. *Cell Motil. Cytoskelet.* **1987**, *8*, 68–75. [CrossRef] [PubMed]
54. Haas, M.; McBrayer, D.; Lytle, C. [Cl-]i-dependent Phosphorylation of the Na-K-Cl Cotransport Protein of Dog Tracheal Epithelial Cells. *J. Biol. Chem.* **1995**, *270*, 28955–28961. [CrossRef] [PubMed]
55. Piala, A.T.; Moon, T.M.; Akella, R.; He, H.; Cobb, M.H.; Goldsmith, E.J. Chloride Sensing by WNK1 Involves Inhibition of Autophosphorylation. *Sci. Signal.* **2014**, *7*, ra41. [CrossRef] [PubMed]
56. Xu, B.-E.; English, J.M.; Wilsbacher, J.L.; Stippec, S.; Goldsmith, E.J.; Cobb, M.H. WNK1, a Novel Mammalian Serine/Threonine Protein Kinase Lacking the Catalytic Lysine in Subdomain II. *J. Biol. Chem.* **2000**, *275*, 16795–16801. [CrossRef] [PubMed]
57. Terker, A.S.; Zhang, C.; Erspamer, K.J.; Gamba, G.; Yang, C.-L.; Ellison, D.H. Unique chloride-sensing properties of WNK4 permit the distal nephron to modulate potassium homeostasis. *Kidney Int.* **2016**, *89*, 127–134. [CrossRef]
58. Murthy, M.; Kurz, T.; O'Shaughnessy, K.M. WNK signalling pathways in blood pressure regulation. *Cell. Mol. Life Sci.* **2016**, *74*, 1261–1280. [CrossRef]
59. Yang, C.-L.; Liu, X.; Paliege, A.; Zhu, X.; Bachmann, S.; Dawson, D.C.; Ellison, D.H. WNK1 and WNK4 modulate CFTR activity. *Biochem. Biophys. Res. Commun.* **2007**, *353*, 535–540. [CrossRef]
60. Hengl, T.; Kaneko, H.; Dauner, K.; Vocke, K.; Frings, S.; Möhrlen, F. Molecular components of signal amplification in olfactory sensory cilia. *Proc. Natl. Acad. Sci. USA* **2010**, *107*, 6052–6057. [CrossRef]
61. Ring, A.M.; Cheng, S.X.; Leng, Q.; Kahle, K.T.; Rinehart, J.; Lalioti, M.D.; Volkman, H.M.; Wilson, F.H.; Hebert, S.C.; Lifton, R.P. WNK4 regulates activity of the epithelial Na+ channel in vitro and in vivo. *Proc. Natl. Acad. Sci. USA* **2007**, *104*, 4020–4024. [CrossRef] [PubMed]
62. Farfel, Z.; Mayan, H.; Yaacov, Y.; Mouallem, M.; Shaharabany, M.; Pauzner, R.; Kerem, E.; Wilschanski, M. WNK4 regulates airway Na+ transport: Study of familial hyperkalaemia and hypertension. *Eur. J. Clin. Invest.* **2005**, *35*, 410–415. [CrossRef] [PubMed]
63. Yasuda, M.; Niisato, N.; Miyazaki, H.; Iwasaki, Y.; Hama, T.; Dejima, K.; Hisa, Y.; Marunaka, Y. Epithelial Na+ channel and ion transport in human nasal polyp and paranasal sinus mucosa. *Biochem. Biophys. Res. Commun.* **2007**, *362*, 753–758. [CrossRef] [PubMed]
64. Chen, J.-C.; Lo, Y.-F.; Lin, Y.-W.; Lin, S.-H.; Huang, C.-L.; Cheng, C.-J. WNK4 kinase is a physiological intracellular chloride sensor. *Proc. Natl. Acad. Sci. USA* **2019**, *116*, 4502–4507. [CrossRef] [PubMed]
65. Anselmo, A.N.; Eamest, S.; Chen, W.; Juang, Y.C.; Kim, S.C.; Zhao, Y.M.; Cobb, M.H. WNK1 and OSR1 regulate the Na+, K+, 2Cl- cotransporter in Hela cells. *Proc. Natl. Acad. Sci. USA* **2006**, *103*, 10883–10888. [CrossRef]
66. Hadchouel, J.; Ellison, D.H.; Gamba, G. Regulation of Renal Electrolyte Transport by WNK and SPAK-OSR1 Kinases. *Annu. Rev. Physiol.* **2016**, *78*, 367–389. [CrossRef]

67. Bazua-Valenti, S.; Gamba, G. Revisiting the NaCl cotransporter regulation by with-no-lysine kinases. *Am. J. Physiol. Cell Physiol.* **2015**, *308*, C779–C791. [CrossRef]
68. Shpetner, H.S.; Paschal, B.M.; Vallee, R.B. Characterization of the microtubule-activated ATPase of brain cytoplasmic dynein (MAP 1C). *J. Cell Biol.* **1988**, *107*, 1001–1009. [CrossRef]
69. Treharne, K.J.; Marshall, L.J.; Mehta, A. A novel chloride-dependent GTP-utilizing protein kinase in plasma membranes from human respiratory epithelium. *Am. J. Physiol. Cell. Mol. Physiol.* **1994**, *267*, L592–L601. [CrossRef]
70. Hirosue, S.; Senn, K.; Clement, N.; Nonnenmacher, M.; Gigout, L.; Linden, R.M.; Weber, T. Effect of inhibition of dynein function and microtubule-altering drugs on AAV2 transduction. *Virology* **2007**, *367*, 10–18. [CrossRef]
71. Yasuda, M.; Niisato, N.; Miyazaki, H.; Hama, T.; Dejima, K.; Hisa, Y.; Marunaka, Y. Epithelial Ion Transport of Human Nasal Polyp and Paranasal Sinus Mucosa. *Am. J. Respir. Cell Mol. Biol.* **2007**, *36*, 466–472. [CrossRef] [PubMed]